RAA 2019 Vol. 19 No. 2, 27(10pp) doi: 10.1088/1674–4527/19/2/27

http://www.raa-journal.org http://iopscience.iop.org/raa

Research in Astronomy and Astrophysics

Variation of physical properties across the green valley for local galaxies

Xue Ge, Qiu-Sheng Gu, Yong-Yun Chen and Nan Ding

School of Astronomy and Space Science, Nanjing University, Nanjing 210093, China; *qsgu@nju.edu.cn*
Key Laboratory of Modern Astronomy and Astrophysics, Nanjing University, Nanjing 210093, China
Collaborative Innovation Center of Modern Astronomy and Space Exploration, Nanjing 210093, China

Received 2018 May 21; accepted 2018 August 2

Abstract We selected a sample of nearby galaxies from the Sloan Digital Sky Survey Data Release 7 (SDSS DR7) to investigate the variation of physical properties from the blue cloud to green valley to red sequence. The sample is limited to a narrow range in the color-stellar mass diagram. After splitting green valley galaxies into two parts—a bluer green valley (green 1) and a redder one (green 2) and three stellar mass bins, we investigate the variation of physical properties across the green valley region. Our main results are as follows: (i) The percentages of pure bulge and bulge-dominated/elliptical galaxies increase gradually from blue cloud to red sequence while the percentages of pure disk and disk-dominated/spiral galaxies decrease gradually in all stellar mass bins and different environments. (ii) With the analysis of morphological and structural parameters (e.g., concentration (C) and the stellar mass surface density within the central 1 kpc (Σ_1)), red galaxies show more luminous and compact cores than both green valley and blue galaxies, while blue galaxies show the opposite behavior in all stellar mass bins. (iii) A strong negative (positive) relationship between bulge-to-total light ratio (B/T) and specific star formation rate (sSFR) (D_{4000}) is found from blue to red galaxies. Our results indicate that the growth in bulge plays an important role when the galaxies change from the blue cloud, to the green valley and to the red sequence.

Key words: galaxies: structure — galaxies: star formation — galaxies: bulges

1 INTRODUCTION

A bimodal distribution of optical color (Strateva et al. 2001; Blanton et al. 2003), ultraviolet (UV)-optical color (Salim et al. 2007), morphology (Driver et al. 2006) or star formation rate (SFR) (Kauffmann et al. 2003a,b) of galaxies has been unambiguously observed. In color-magnitude diagrams (CMDs), the galaxies are divided into “red sequence” and “blue cloud.” Generally speaking, red sequence contains old and quiescent galaxies (Kauffmann et al. 2003a), while blue cloud mainly contains blue star-forming disk galaxies (Kaviraj 2014a,b). The galaxies between red sequence and blue cloud are called “green valley” cases, which are considered as a transition population. Wyder et al. (2007) and Jin et al. (2014) found that a two-Gaussian fitting to the galaxies in the CMD is not sufficient which suggests that the green valley is not a simple mixture of red sequence and blue cloud. Therefore, green valley galaxies can provide us with crucial clues to connect the red sequence and blue cloud in terms of star formation quenching and evolution of galaxies.

Previous studies have shown that since $z \sim 1$ the number and stellar mass of blue galaxies are almost constant while the stellar mass of red galaxies has increased by a factor of $2 \sim 4$ (Bell et al. 2004; Faber et al. 2007). This scenario supports that the existence of red galaxies requires certain quenching mechanisms to stop or weaken the star formation in blue galaxies (Bell et al. 2004). Different quenching mechanisms have been proposed to explain the transition from blue to red galaxies, such as major mergers (Springel et al. 2005; Di Matteo et al. 2005), AGN and supernova feedback (Di Matteo et al. 2005; Nandra et al. 2007; Marasco et al. 2012), morphological quenching (Martig et al. 2009, 2013) and environmental quenching (Peng et al. 2010).

The quenching mechanisms mentioned above impose restrictions on galaxy structure. These restrictions provide us with an additional approach to understand the connection between the changes of galaxy structure and the location in which a galaxy resides. For example, elliptical galaxies are more concentrated due to internal or external processes than spiral galaxies. This provides a motivation for us to explore the connection between the morphology/structure and star formation activity. Pan et al. (2013) have shown that green valley galaxies have a lower (higher) Gini coefficient (G) (second order moment ($M20$)) than red galaxies but higher (lower) G ($M20$) than blue galaxies. The average value of asymmetry parameter (A) for green valley galaxies is also between that of both red and blue galaxies. Moreover, the strong connection between morphological/structural parameters and star formation activity has been demonstrated in the studies utilizing local galaxy surveys (Kauffmann et al. 2003b; Mendez et al. 2011; Fang et al. 2013). Some structural thresholds, such as critical stellar mass, stellar surface mass density and Sérsic index, reflect the transformation from blue galaxies to red galaxies. Galaxies above these thresholds tend to be old or quiescent while galaxies tend to be young or active below these thresholds (Kauffmann et al. 2003b; Driver et al. 2006; Schiminovich et al. 2007; Bell 2008). Cheung et al. (2012) and Fang et al. (2013) used a structural parameter, Σ_1 (the stellar mass surface density within the central 1 kpc), to investigate whether there is a difference between different galaxy colors, and found Σ_1 is a better indicator for the sequence of galaxies than other parameters. Bait et al. (2017) employed multiwavelength data to study the dependence of star formation on morphology and environment in the local universe. Their results suggested that the morphology of galaxies correlates with star formation although environmental effects on morphology are weak.

This work will focus on the variation of physical properties from blue cloud to green valley to red sequence in a narrow range of optical color and different stellar mass bins. In particular, we attempt to investigate whether there is a monotonic variation in morphology/structure and star formation, so we split green valley galaxies into two populations (i.e., green 1 and green 2). We also expect to have a further understanding of the environmental effects on star formation activity in the local universe.

The outline of the paper is as follows. In Section 2, we introduce our sample selection and data. The results and discussions are presented in Sections 3 and 4 respectively. Finally, we present our conclusions in Section 5. The cosmological constants adopted in this work are $\Omega_m = 0.3, \Omega_\Lambda = 0.7$ and $H_0 = 70\,\mathrm{km}^{-1}\,\mathrm{s}^{-1}\,\mathrm{Mpc}^{-1}$.

2 SAMPLE AND DATA

Meert et al. (2015) and Meert et al. (2016) presented a catalog containing 670 722 galaxies selected from the Sloan Digital Sky Survey Data Release 7 (SDSS DR7) (York et al. 2000; Abazajian et al. 2009). These galaxies were chosen based on three criteria: (1) $14 < r$ band Petrosian magnitude <17.7 after the Galaxy extinction correction; (2) the object should be a galaxy as identified by the photo pipeline; (3) the spectrum of the object is recognized as a galaxy. Each galaxy was fitted by using four models (de Vacouleurs (Dev), Sérsic (Ser), de Vacouleurs+Exponential (DevExp) and Sérsic+Exponential (SerExp) profiles) with the point spread function being corrected in g, r and i bands. The routine Galfit (Peng et al. 2002) and analysis pipeline PyMorph (Vikram et al. 2010) were used for the fitting. We choose the SerExp model where a galaxy was fitted with two components (bulge and disk). We select the galaxies with $n < 8$ (the Sérsic index of bulge), $b/a > 0.63$ (the ratio of minor axis to major axis) in g, r and i bands and flag bits 1–13 in the r band (Meert et al. 2015, 2016). In order to acquire k-corrected Petrosian magnitudes, we cross match the catalog with the New York University Value-Added Catalog (Blanton et al. 2005) and derive a preliminary sample containing 155 388 galaxies.

Figure 1 shows the preliminary sample selected according to the above criteria. To ensure a broader span of luminosity and completeness of color in each magnitude bin, we divide galaxies into 12 bins from $M_{r,0.1} = -18.50 \sim -21.5$ mag and $0.02 < z < 0.18$ with bin size of 0.25 mag, as shown in Figure 1 ($M_{r,0.1}$ is the absolute magnitude in r band k-corrected to $z = 0.1$). The sources with quite high or low r band absolute magnitudes are excluded and we use only the sources in red boxes to produce the final sample.

Figure 2 shows the distribution of color-stellar mass for galaxies selected in Figure 1. $(u-r)_{0.1}$ is the color that is k-corrected to $z = 0.1$ and stellar masses are obtained from MPA/JHU[1] (Kauffmann et al. 2003a). We select the sources with $(u-r)_{0.1}$ color from 1.75 to 2.25 and stellar mass from 10.2 to 11.1 (in logarithm scale) as our final sample. We define the galaxies with $(u-r)_{0.1}$ color between 1.75 and 1.85, between 1.85 and 2.0, between 2.0 and 2.15 and between 2.15 and 2.25 as blue galaxies, green 1 galaxies, green 2 galaxies and red galaxies respectively. Further, the stellar mass is split into three ranges (i.e., [10.2,10.5], [10.5,10.8], [10.8,11.1]) to investigate the role stellar mass plays when the blue galaxies go through

[1] *http://www.mpa-garching.mpg.de/SDSS/DR7/*

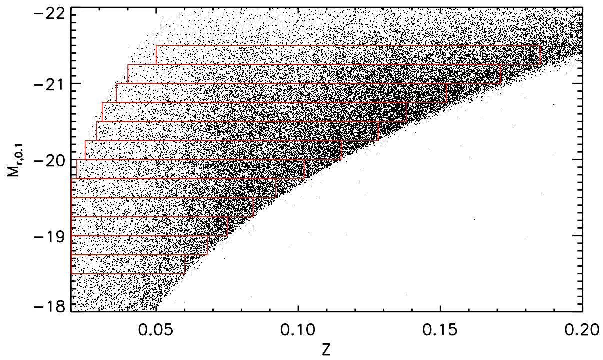

Fig. 1 The preliminary sample distribution (*black points*) in the r band absolute magnitude and z space. $M_{r,0.1}$ is the absolute magnitude which is k-corrected to $z = 0.1$ in r band. We only select objects in *red boxes* to produce the final sample analyzed in this paper.

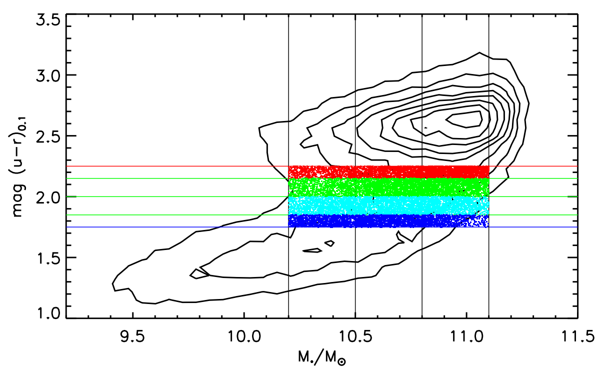

Fig. 2 The distribution of color-stellar mass for galaxies in *red boxes* in Fig. 1. $(u-r)_{0.1}$ is the color that is k-corrected to $z = 0.1$. The galaxies with $(u-r)_{0.1}$ color between 1.75 and 1.85 (*blue points*), 1.85 and 2.0 (*cyan points*), 2.0 and 2.15 (*green points*) and 2.15 and 2.25 (*red points*) are defined as blue galaxies, green 1 galaxies, green 2 galaxies and red galaxies respectively. The *vertical lines* represent different stellar mass bins.

the green valley into the red sequence. Table 1 provides information on the final sample. Considering the contamination of dusty star-forming galaxies to green valley galaxies, we estimate the fraction of dusty green valley galaxies in our sample based on *WISE* mid-infrared (Cutri & et al. 2014) and *GALEX* near-UV (Martin et al. 2005) catalogs. The dusty star-forming galaxies are defined as galaxies with $f_{12\,\mu\mathrm{m}}/f_{\mathrm{nuv}} > 200$ and $f_{4.6\,\mu\mathrm{m}}/f_{3.4\,\mu\mathrm{m}} > 0.85$ (Yesuf et al. 2014). We find only 2 percent of dusty star-forming galaxies is in the green valley, which is negligible and will not affect our results significantly.

Physical parameters include: morphological parameters (concentration (C), $M20$ and G) and structural parameters (n and bulge-to-total light ratio (B/T)) obtained from Meert et al. (2015), specific star formation rate (sSFR) and D_{4000} obtained from the MPA/JHU catalog.

Table 1 The Galaxies in Our Final Sample

Galaxy type (1)	log M_* (2)	$(u-r)_{0.1}$ (3)	Number (4)
Blue	[10.2 – 10.5]	[1.75 – 1.85]	1110
	[10.5 – 10.8]	[1.75 – 1.85]	1263
	[10.8 – 11.1]	[1.75 – 1.85]	692
Green 1	[10.2 – 10.5]	[1.85 – 2.0]	1273
	[10.5 – 10.8]	[1.85 – 2.0]	1668
	[10.8 – 11.1]	[1.85 – 2.0]	1328
Green 2	[10.2 – 10.5]	[2.0 – 2.15]	938
	[10.5 – 10.8]	[2.0 – 2.15]	1625
	[10.8 – 11.1]	[2.0 – 2.15]	1682
Red	[10.2 – 10.5]	[2.15 – 2.25]	689
	[10.5 – 10.8]	[2.15 – 2.25]	1160
	[10.8 – 11.1]	[2.15 – 2.25]	1491

Notes: Col. (1) Galaxy type; Col. (2) Stellar mass range; Col. (3) $(u-r)_{0.1}$ color which is k-corrected to $z = 0.1$; Col. (4) Galaxy number.

3 RESULTS

3.1 Morphological Distribution

We separate galaxies into five morphologies based on the flagged system in Meert et al. (2015). In the flagged system, bulge galaxies and disk galaxies have flag bits 1 and 4 set respectively. Two-component galaxies have flag bits set to 10. For bulge galaxies, we define galaxies with flag bits set to 2 as pure bulge while those with flag bits set to 3 as bulge-dominated. For disk galaxies, pure disk and disk-dominated galaxies have flag bits set to 5 and set to 6, 7, 8 and 9 respectively. The remaining galaxies are defined as two-component galaxies.

Figure 3 shows the distributions of different morphologies in different stellar mass bins. We can see clearly that the fractions of pure bulge and bulge-dominated galaxies increase gradually while the fractions of pure disk and disk-dominated galaxies decrease gradually from blue to green to red galaxies in all stellar mass bins. What is more, it is found that the percentage of bulge galaxies appears to have an increasing tendency from low to high stellar mass bins which is independent of the galaxy colors. In contrast, the percentage of disk galaxies shows a decreasing tendency as we move from low to high stellar mass ranges. Obviously, these variations will lead to the build-up of massive bulge galaxies and the insufficiency of massive disk galaxies.

Many previous studies involving the multi-component decomposition of a large sample of galaxies (Simard et al. 2011; Lackner & Gunn 2012; Meert et al. 2015, 2016) are model-dependent. So, we cross match our sample with the catalog of Galaxy Zoo 1 (Lintott et al. 2011), in which the

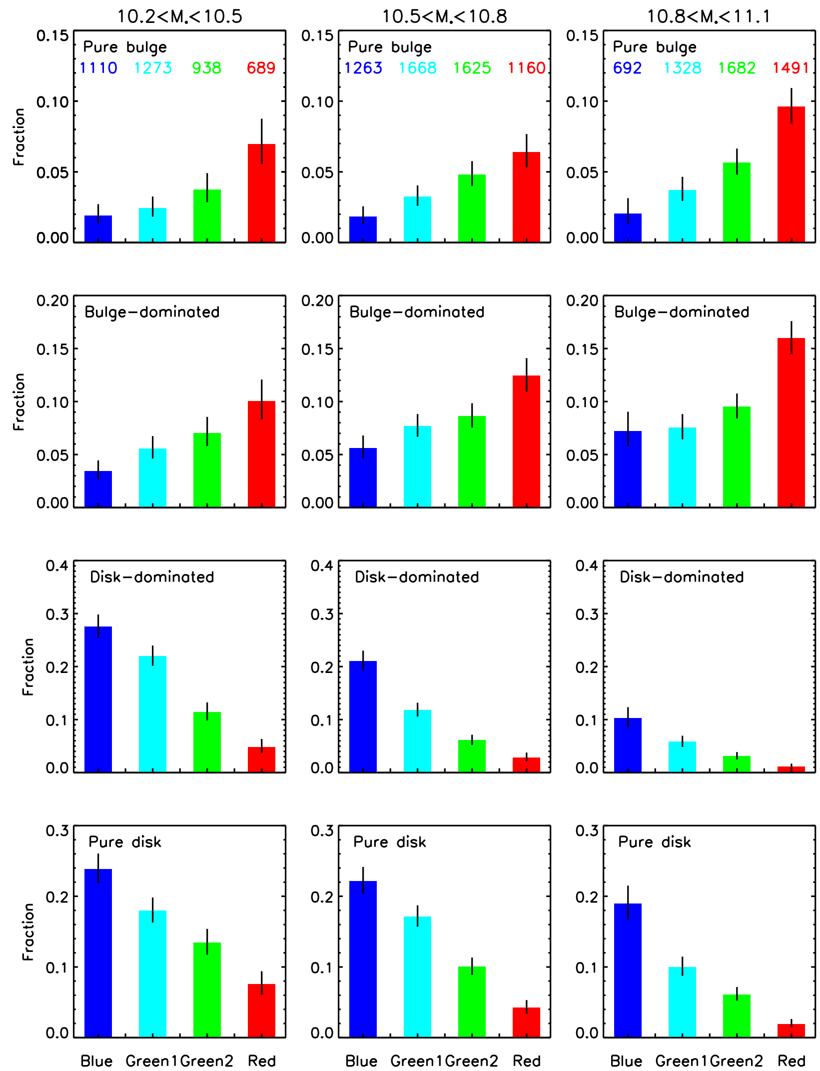

Fig. 3 The fractions of different morphologies (from top to bottom: pure bulge, bulge-dominated, disk-dominated and pure disk respectively) for blue, green 1, green 2 and red galaxies in $10.2 < \log M_* < 10.5$ (*left*), $10.5 < \log M_* < 10.8$ (*middle*) and $10.8 < \log M_* < 11.1$ (*right*). The identification of different morphologies is from the bulge and disk decomposition. The *black vertical lines* are the binomial error of fraction (Cameron 2011). The number of galaxy types in each stellar mass bin is marked on the top (see also Table 1).

morphological classifications of all galaxies with $0.001 < z < 0.25$ from SDSS DR7 are listed. Six morphologies (Elliptical galaxy, Clockwise/Z-wise spiral galaxy, Anti-clockwise/S-wise spiral galaxy, Spiral galaxy other, Star or Unknown and Merger) based on visual classifications were derived and each object was classified as a possible morphology 38 times on average by thousands of volunteers. We combine Clockwise/Z-wise spiral galaxy, Anti-clockwise/S-wise spiral galaxy and Spiral galaxy other as spiral classification. Moreover, Yang et al. (2007) provided a catalog of environments where the masses of dark matter halos for SDSS DR4 galaxies have been estimated. We follow the way described by van den Bosch (2002) and define the environment of galaxies based on dark matter halo masses. A galaxy is defined as a field galaxy, group galaxy or cluster galaxy if its dark matter halo mass is less than $10^{13}\,M_\odot$, between $10^{13}\,M_\odot$ and $10^{14}\,M_\odot$ or higher than $10^{14}\,M_\odot$, respectively. We do not choose a threshold to classify a galaxy as an elliptical or spiral considering that a conservative threshold can significantly reduce the number of samples. Actually, the medians of votes that have been corrected for classification bias (Bamford et al. 2009) can also reflect the morphologies of galaxies.

Figure 4 displays the relationship between the medians of votes and environments for different galaxy sequences. We conclude that blue galaxies have a higher probability of being classified as spiral galaxies while red galaxies have a higher probability of being classified as elliptical galaxies. The median probabilities of being spiral or elliptical for green 1 and green 2 galaxies are between blue and red galaxies. This result is consistent with Figure 3. It can be noted that we have demonstrated that the variation of morphological distribution is independent of stellar mass (Fig. 3). So in Figure 4, we do not split galaxies into different stellar mass bins. We do not find that the environment can strongly change the probability of being a morphological classification. For different environments, it is found that the fraction of green valley galaxies is approximately constant at 57–61 percent although we select only a part of the blue and red galaxies. In addition, the ratio of blue to green valley galaxies decreases significantly with environmental richness (from 38 percent in a field case to 20 percent in a cluster case). These results support the notion that while environment does not affect significantly the morphological distribution of galaxies and the timescale for crossing the green valley, it can aid the process by which galaxies start to evolve from blue cloud to red sequence (Bremer et al. 2018).

It is widely accepted that blue galaxies are active star-forming galaxies and that most of them are dominated by disks. On the other hand, red galaxies are quiescent elliptical galaxies with compact cores. Green valley galaxies have morphological properties intermediate between blue and red galaxies. The conclusions above are consistent with Coenda et al. (2018) and the variation of morphology is monotonic from blue to green 1 to green 2 to red galaxies.

3.2 Morphological and Structural Parameters

Many previous works claimed that early type galaxies (ETGs) and late type galaxies (LTGs) have different distributions in G and A diagrams (Abraham et al. 1996; Lotz et al. 2004; Kong et al. 2009). These results argued that ETGs have higher G and lower A than LTGs. In order to further confirm the tendency of variation for these parameters, we investigate the variation of morphological parameters including C, $M20$ and G (Fig. 5). Parameter C quantifies the concentration of starlight in a galaxy. $M20$ and G represent the second order moment of the brightness for 20 percent of pixels and the light distribution of pixels in a galaxy (see the detailed definition in Lotz et al. 2004) respectively. We find a graded variation tendency from blue to green 1 to green 2 to red galaxies in all stellar mass bins. For example, the median of C changes from 2.41 to 2.59, from 2.50 to 2.67, and from 2.59 to 2.80 in three stellar mass bins respectively. In the entire blue, green valley and red galaxies, the median is from 2.48 to 2.72. This tendency of variation is found not only in C but also in $M20$ and G. The Kolmogorov-Smirnov (K-S) test shows these distributions have a significant difference with $p \ll 0.0001$. We can conclude that the variation of these morphological parameters results from the prominence of galactic nuclei.

The NASA-Sloan Atlas[2] provides the surface brightness profiles of SDSS local galaxies in u, g, r, i, z bands in a series of angular sizes. In this work, we compute stellar mass surface density profiles, Σ_1, utilizing this catalog. The computational process is listed in the following steps. First, the cumulative light profile in the i band is fitted through spline algorithms which allows us to obtain the interpolated light profile at 1 kpc. Second, the light within the central 1 kpc is corrected by using SDSS Galactic extinction and the k-correction calculator of Chilingarian et al. (2010). Finally, the surface brightness within the central 1 kpc is converted into mass density through the mass-to-light ratio (M/L) in the i band. The stellar masses in M/L are obtained from the MPA/JHU catalog (Kauffmann et al. 2003a). Population properties, such as metallicity and initial mass function, may affect the accuracy of M/L. However, Fang et al. (2013) suggested that metallicity has nearly no effect on the measurement of M/L. The initial mass function would lead to an underestimate of Σ_1 for massive red galaxies, which would be in line with our expectations.

In addition to Σ_1, we also investigate the variation of other structural parameters including n and B/T. Figure 6 shows the distributions of these parameters in different stellar mass bins. We find blue galaxies have the lowest medians of these parameters while red galaxies have the highest values and this phenomenon is independent of stellar mass. The K-S test with $p \ll 0.0001$ shows these parameters have different distributions. The continuous variation tendency from blue to green 1 to green 2 to red galaxies reflects a criterion in which the bulge component is more and more distinct, which indicates that bulge plays an important role during the transformation from blue cloud to red sequence.

3.3 B/T and sSFR

In order to investigate the relationship between bulge and star formation activity from blue to red galaxies, we select two groups of additional blue galaxies and two groups of additional red galaxies.

[2] *http://www.sdss.org/dr14/manga/manga-target-selection/nsa/*

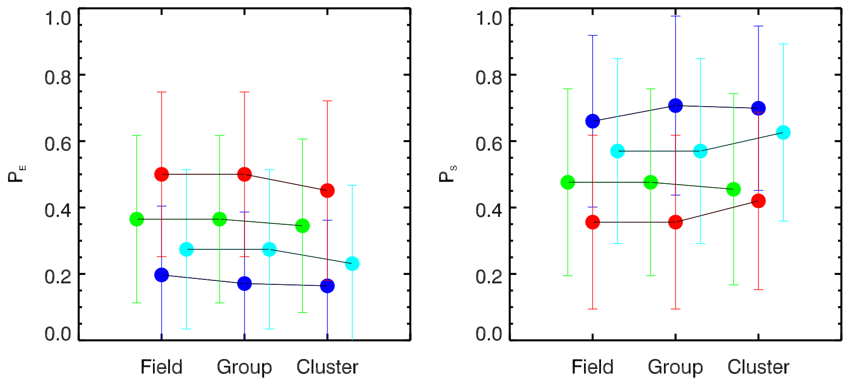

Fig. 4 Median probabilities of elliptical (*left*) and spiral (*right*) vs. different environments. Blue galaxies, green 1 galaxies, green 2 galaxies and red galaxies are marked with *blue*, *cyan*, *green* and *red solid circles* respectively. In each panel, the standard deviations are expressed as the errors of median probabilities. *Green* and *cyan points* are shifted by 0.03 along the x-axis.

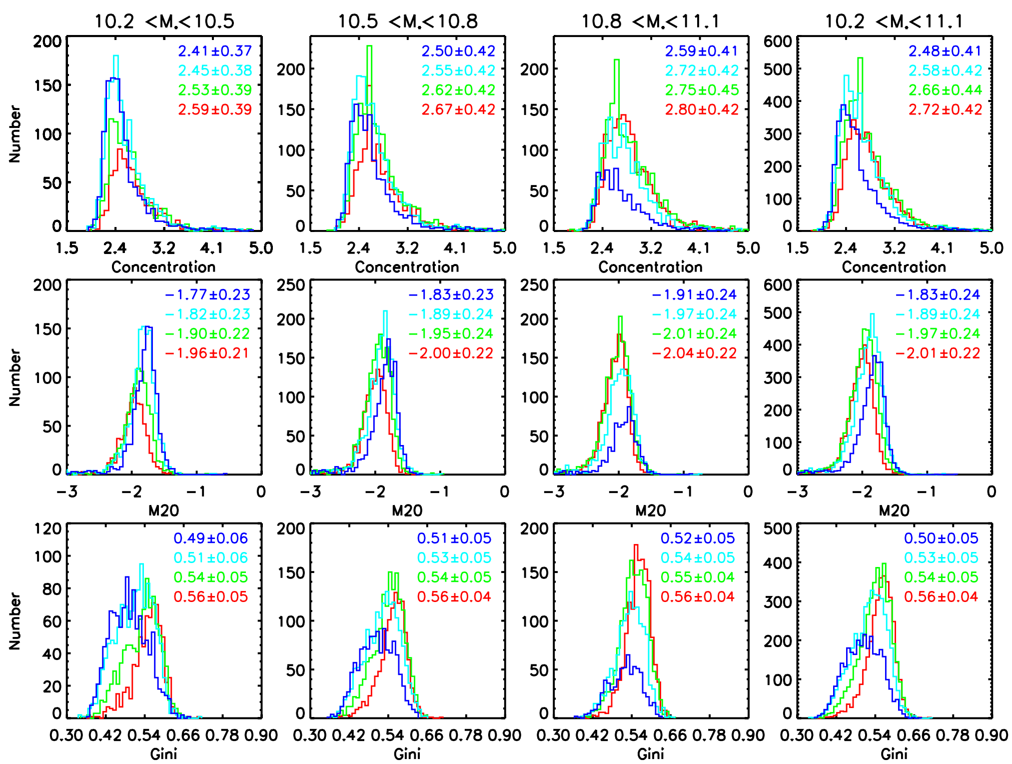

Fig. 5 The distributions of different morphological parameters including C, $M20$ and G (from top to bottom respectively) in $10.2 < \log M_* < 10.5$, $10.5 < \log M_* < 10.8$, $10.8 < \log M_* < 11.1$ and $10.2 < \log M_* < 11.1$ (from left to right respectively). *Blue*, *cyan*, *green* and *red histograms* represent blue, green 1, green 2 and red galaxies respectively. The corresponding medians and standard deviations are labeled on the top-right corners.

Figure 7 displays the reconstructed sample where purple, blue, yellow and red points are the additional sources used next. It can be noted that the stellar mass range for purple and blue points is from 9.9 to 10.8 in logarithm scale because of the lack of massive blue galaxies.

In Figure 8 (left), we show the relationship between median B/T and sSFR. The solid black line in the panel is the best fit. The formula for the best fit is

$$B/T = -1.65(\pm 0.08) - 0.20(\pm 0.01) \log \mathrm{sSFR}\,. \quad (1)$$

We can see from the picture that B/T increases as sSFR decreases from blue to red galaxies. Moreover, massive galaxies have a lower sSFR and higher B/T in the same $u - r$ color in general. We find that the extremely blue galaxies (blue and purple) do not follow this tendency. We contribute the deviation to the scatter of bulge-disk decomposition due to the inapparent bulges in extremely blue galaxies. sSFR used in this paper is computed by different methods (Brinchmann et al. 2004), which can generate

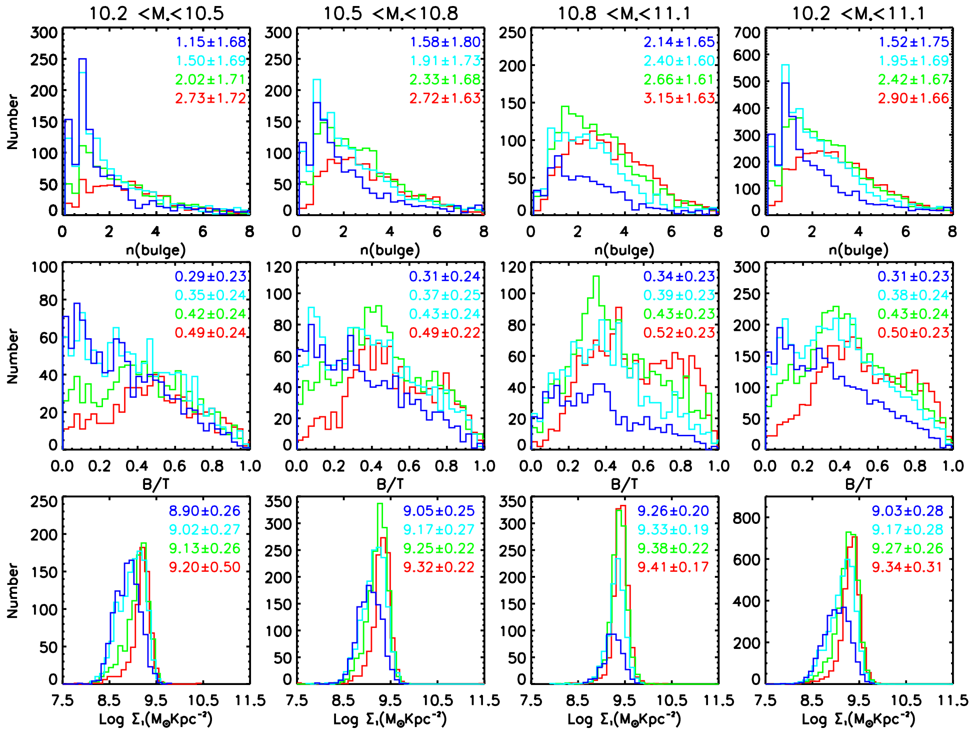

Fig. 6 The distributions of structural parameters including n, B/T and Σ_1 (from top to bottom respectively). All colors and labels are the same as in Fig. 5.

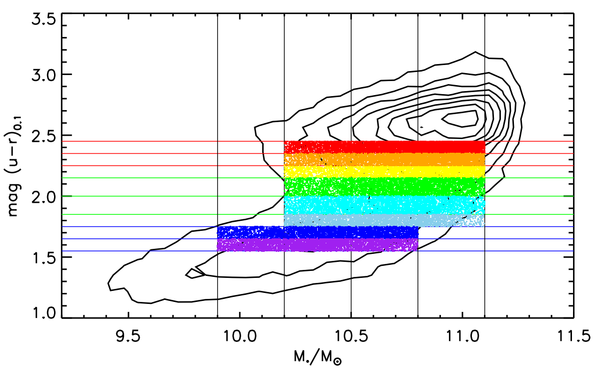

Fig. 7 Reconstructed sample containing three groups of blue galaxies (*purple*, *dark blue* and *light blue*), two groups of green valley galaxies (*cyan* and *green*) and three groups of red galaxies (*yellow*, *orange* and *red*) in the color-stellar mass diagram.

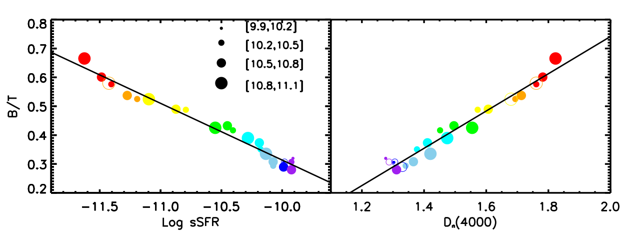

Fig. 8 The relationships between B/T and sSFR (*left*) / D_{4000} (*right*). The size and color of circles represent the stellar mass and range of $u - r$ respectively. Some points are marked with *open circles* because of overlap with the *solid points*. The *solid black line* in each panel represents the best fit.

some biases. As a substitute for sSFR, we show the relationship between median B/T and D_{4000} (Fig. 8, right). D_{4000} is defined as the ratio of continuum 3850–3950 Å to 4000–4100 Å (Balogh et al. 1999) and is a good indicator for galaxy age, so it reflects recent star formation activity in galaxies. A strong positive correlation is found between them. The formula for the best fitting is

$$B/T = -0.55(\pm 0.05) + 0.64(\pm 0.03) D_{4000}\,. \quad (2)$$

sSFR or D_{4000} can be considered as a proxy for recent star-forming. Lower sSFR or higher D_{4000} suggests an older stellar population. As we can see from Figure 8, a galaxy with redder color and higher stellar mass has lower sSFR, which coincides with the build-up of bulge component. Our result is consistent with Salim et al. (2009) who found that sSFR exhibits a continuous and smooth change in sSFR and rest-frame UV-optical color space in local galaxies.

4 DISCUSSION

Various studies have suggested that the morphology of galaxies (e.g., prominent bulge) correlates with star formation history.

Simulations have shown that major mergers can lead to a starburst in the centers of galaxies by sweeping gas into the center (Di Matteo et al. 2005). The starburst consumes gas rapidly, which leads to growth of the bulge and ultimately changes the morphology (Springel et al. 2005; Hopkins et al. 2010; Cheung et al. 2012). Red galaxies have a higher proportion of bulge/elliptical galaxies in our study, which suggests that the prominent bulge in red galaxies may play an important role during the process of preventing star formation. For example, the existence of a stellar spheroid is responsible for the stability of disks, thus opposing gravitational instability to form stars (Martig et al. 2009, 2013). Cheung et al. (2012) and Fang et al. (2013) investigated the relationship between quenching mechanisms and galaxy structural parameters. They found that red galaxies have the highest Σ_1 and blue galaxies have the lowest value on average. Green valley galaxies are between blue and red galaxies. The suggestion they proposed was that Σ_1 may be more physically connected with the quenching process. However, the threshold is only a necessary condition in the quenching process. The connection between bulge growth and star formation quenching remains an unanswered question. Combining low-z with high-z galaxies drawn from GAMA and CANDELS respectively, Brennan et al. (2017) studied the connection between the location relative to the star formation main sequence (SFMS) and structural parameters. Based on a semi-analytic model in which formation of a bulge occurred not only due do merger events but also disk instabilities, they found that star formation activity was strongly associated with build-up of a bulge component.

Our analysis based on the decomposition of bulge and disk and morphological/structural parameters shows that the bulge component is more and more prominent when we go from blue to green 1 to green 2 to red galaxies. The monotonic variation is reflected through the largest Σ_1, n and B/T in red galaxies and smallest ones in blue galaxies. In addition, when we expand the sample, strong correlations between B/T and sSFR/D_{4000} demonstrate that the recession of star formation is strongly correlative with the build-up of a bulge. Although not all red galaxies have a prominent bulge component, we can conclude that the recession of star formation is accompanied by the build-up of a bulge, as described in Bell et al. (2012) and Lang et al. (2014), who argued that a prominent bulge is a better indicator for the quenching of star formation. Our results in this work are consistent with those in Brennan et al. (2017) who also found a tendency for monotonic variation in galaxy structural parameters with changes in the location relative to SFMS.

We combine the morphological classification of Galaxy Zoo (Lintott et al. 2011) with the environment catalog (Yang et al. 2007) and investigate the effects of environment on morphologies. Our result shows that the morphology is almost independent of the environment, which is consistent with Coenda et al. (2018). Furthermore, the stellar mass of our sample is $> 10^{10}\,M_\odot$. It is not strange that the quenching mode is more dependent on internal processes rather than external processes (Peng et al. 2010). We find the ratio between green valley galaxies and total galaxies is approximately constant at 58 percent in different environments, although we do not include all blue and red galaxies in our sample. It can be noted that the result is consistent with Bremer et al. (2018) who used $u - r$ color and stellar mass to define green valley galaxies. They found the ratio of green valley galaxies to the whole sample is approximately 18 percent at a given environmental richness. Bait et al. (2017) concluded that the fraction of green valley galaxies is almost constant (20 percent) in all environments based on the selection of sSFR. The invariable fraction indicates that the environment cannot change the timescale for crossing the green valley. Many previous studies have indicated the transition timescale is $\sim$1 Gyr, otherwise we cannot see a bimodal distribution in the CMD diagram (Faber et al. 2007; Balogh et al. 2011).

It has been known that stellar mass is strongly related to SFR in the local and high-z universe (Brinchmann et al. 2004; Salim et al. 2007; Elbaz et al. 2007; Peng et al. 2010). In this paper, the galaxies are divided into three stellar mass bins (i.e., $10.2 < \log M_* < 10.5$, $10.5 < \log M_* < 10.8$, $10.8 < \log M_* < 11.1$). We find the fractions of pure bulge and bulge-dominated galaxies are slightly higher in cases with larger stellar mass than those in smaller stellar mass. Simultaneously, pure disk and disk-dominated galaxies more easily exhibit low stellar mass (see Fig. 3). The reduction of blue pure disk and disk-dominated galaxies coincides with the build-up of red pure bulge and bulge-dominated galaxies. This provides us with insight into the evolution of a galaxy from blue to red. Faber et al. (2007) proposed a "mixed" model for the formation of spheroidal galaxies. In the model, the quenching process can occur very early or late. In short, blue star-formation galaxies can quench to red massive galaxies in two ways. The first is very early quenching at low stellar mass such that fewer galaxies remain blue when reaching the high stellar mass region. The second is very late quenching which occurs shortly after reaching a sufficiently high stellar mass.

In Figures 5 and 6, the medians of morphological and structural parameters have a slight rise or decline from low to high stellar mass. It indicates that for galaxies with the same color, massive galaxies have a more prominent bulge component (see also Fig. 8). Red galaxies have more prominent bulge properties in regions with higher stellar mass. It seems that galaxies within the high stellar mass range quench preferentially which will lead to increasing the number of massive red galaxies. Furthermore, less massive star forming galaxies will shut down their starforming in a later epoch and shift to the end of massive quenching galaxies. This is consistent with the criterion of "Downsizing" (Cowie et al. 1996).

5 CONCLUSIONS

Using a sample drawn from SDSS DR7, together with the data from other public catalogs, we have investigated the variation of physical parameters for blue, green 1, green 2 and red galaxies. In addition, we have also discussed the importance of a bulge in quenching star formation. Our main conclusions are as follows:

(1) Blue galaxies have the lowest fraction of bulge/elliptical galaxies and the highest fraction of disk/spiral galaxies. However, the fraction is opposite in red galaxies. Green valley galaxies have an intermediate fraction. The morphologies show continuous change from blue cloud to green valley to red sequence. It is found that the monotonic variation is independent of the stellar mass and environments.

(2) The fraction of green valley galaxies is almost constant while the ratio between blue and green valley galaxies decreases as we move from low to high environmental richness, which indicates that the effects of environment are not on the timescale of crossing the green valley but on the timescale when the blue galaxies start to transform their morphologies.

(3) The medians of morphological parameters (C, $M20$ and G) and structural parameters (n, B/T and Σ_1) show a monotonic decreasing or increasing tendency from blue to green 1 to green 2 to red galaxies, suggesting that the build-up of a bulge component plays an important role during the morphological transformation.

(4) For galaxies with the same color, massive galaxies have a more prominent bulge property. The quenching rate is higher in high environmental richness than that of low environmental richness if we consider the percentage of red galaxies as an indicator for quenching rate in different environments.

(5) Combining additional blue and red galaxies, we find there is a strong negative (positive) relationship between B/T and sSFR (D_{4000}). In the same range of $u - r$ color, massive galaxies have higher B/T when given the sSFR or D_{4000}. The monotonic variation suggests that the physical processes associated with strengthening the bulge are also the ones associated with weakening star formation.

Acknowledgements This work is supported by the National Key Research and Development Program of China (No. 2017YFA0402703) and by the National Natural Science Foundation of China (No. 11733002). Funding for the Sloan Digital Sky Survey (SDSS) has been provided by the Alfred P. Sloan Foundation, the Participating Institutions, the National Science Foundation, the US Department of Energy, the National Aeronautics and Space Administration, the Japanese Monbukagakusho and the Max Planck Society. The SDSS web site is *http://www.sdss.org/*. The SDSS is managed by the Astrophysical Research Consortium for the Participating Institutions. The Participating Institutions are the American Museum of Natural History, Astrophysical Institute Potsdam, University of Basel, Cambridge University, Case Western Reserve University, University of Chicago, Drexel University, Fermilab, the Institute for Advanced Study, the Japan Participation Group, Johns Hopkins University (JHU), the Joint Institute for Nuclear Astrophysics, the Kavli Institute for Particle Astrophysics and Cosmology, the Korean Scientist Group, the Chinese Academy of Sciences (LAMOST), Los Alamos National Laboratory, the Max-Planck-Institute for Astronomy (MPIA), the Max-Planck-Institute for Astrophysics (MPA), New Mexico State University, Ohio State University, University of Pittsburgh, University of Portsmouth, Princeton University, the United States Naval Observatory and the University of Washington.

References

Abazajian, K. N., Adelman-McCarthy, J. K., Agüeros, M. A., et al. 2009, ApJS, 182, 543
Abraham, R. G., Tanvir, N. R., Santiago, B. X., et al. 1996, MNRAS, 279, L47
Bait, O., Barway, S., & Wadadekar, Y. 2017, MNRAS, 471, 2687
Balogh, M. L., Morris, S. L., Yee, H. K. C., Carlberg, R. G., & Ellingson, E. 1999, ApJ, 527, 54
Balogh, M. L., McGee, S. L., Wilman, D. J., et al. 2011, MNRAS, 412, 2303
Bamford, S. P., Nichol, R. C., Baldry, I. K., et al. 2009, MNRAS, 393, 1324
Bell, E. F., Wolf, C., Meisenheimer, K., et al. 2004, ApJ, 608, 752
Bell, E. F. 2008, ApJ, 682, 355

Bell, E. F., van der Wel, A., Papovich, C., et al. 2012, ApJ, 753, 167

Blanton, M. R., Hogg, D. W., Bahcall, N. A., et al. 2003, ApJ, 594, 186

Blanton, M. R., Schlegel, D. J., Strauss, M. A., et al. 2005, AJ, 129, 2562

Bremer, M. N., Phillipps, S., Kelvin, L. S., et al. 2018, MNRAS, 476, 12

Brennan, R., Pandya, V., Somerville, R. S., et al. 2017, MNRAS, 465, 619

Brinchmann, J., Charlot, S., White, S. D. M., et al. 2004, MNRAS, 351, 1151

Cameron, E. 2011, PASA, 28, 128

Cheung, E., Faber, S. M., Koo, D. C., et al. 2012, ApJ, 760, 131

Chilingarian, I. V., Melchior, A.-L., & Zolotukhin, I. Y. 2010, MNRAS, 405, 1409

Coenda, V., Martínez, H. J., & Muriel, H. 2018, MNRAS, 473, 5617

Cowie, L. L., Songaila, A., Hu, E. M., & Cohen, J. G. 1996, AJ, 112, 839

Cutri, R. M., & et al. 2014, VizieR Online Data Catalog, 2328

Di Matteo, T., Springel, V., & Hernquist, L. 2005, Nature, 433, 604

Driver, S. P., Allen, P. D., Graham, A. W., et al. 2006, MNRAS, 368, 414

Elbaz, D., Daddi, E., Le Borgne, D., et al. 2007, A&A, 468, 33

Faber, S. M., Willmer, C. N. A., Wolf, C., et al. 2007, ApJ, 665, 265

Fang, J. J., Faber, S. M., Koo, D. C., & Dekel, A. 2013, ApJ, 776, 63

Hopkins, P. F., Bundy, K., Croton, D., et al. 2010, ApJ, 715, 202

Jin, S.-W., Gu, Q., Huang, S., Shi, Y., & Feng, L.-L. 2014, ApJ, 787, 63

Kauffmann, G., Heckman, T. M., White, S. D. M., et al. 2003a, MNRAS, 341, 33

Kauffmann, G., Heckman, T. M., White, S. D. M., et al. 2003b, MNRAS, 341, 54

Kaviraj, S. 2014a, MNRAS, 437, L41

Kaviraj, S. 2014b, MNRAS, 440, 2944

Kong, X., Fang, G., Arimoto, N., & Wang, M. 2009, ApJ, 702, 1458

Lackner, C. N., & Gunn, J. E. 2012, MNRAS, 421, 2277

Lang, P., Wuyts, S., Somerville, R. S., et al. 2014, ApJ, 788, 11

Lintott, C., Schawinski, K., Bamford, S., et al. 2011, MNRAS, 410, 166

Lotz, J. M., Primack, J., & Madau, P. 2004, AJ, 128, 163

Marasco, A., Fraternali, F., & Binney, J. J. 2012, MNRAS, 419, 1107

Martig, M., Bournaud, F., Teyssier, R., & Dekel, A. 2009, ApJ, 707, 250

Martig, M., Crocker, A. F., Bournaud, F., et al. 2013, MNRAS, 432, 1914

Martin, D. C., Fanson, J., Schiminovich, D., et al. 2005, ApJ, 619, L1

Meert, A., Vikram, V., & Bernardi, M. 2015, MNRAS, 446, 3943

Meert, A., Vikram, V., & Bernardi, M. 2016, MNRAS, 455, 2440

Mendez, A. J., Coil, A. L., Lotz, J., et al. 2011, ApJ, 736, 110

Nandra, K., Georgakakis, A., Willmer, C. N. A., et al. 2007, ApJ, 660, L11

Pan, Z., Kong, X., & Fan, L. 2013, ApJ, 776, 14

Peng, C. Y., Ho, L. C., Impey, C. D., & Rix, H.-W. 2002, AJ, 124, 266

Peng, Y.-j., Lilly, S. J., Kovač, K., et al. 2010, ApJ, 721, 193

Salim, S., Rich, R. M., Charlot, S., et al. 2007, ApJS, 173, 267

Salim, S., Dickinson, M., Michael Rich, R., et al. 2009, ApJ, 700, 161

Schiminovich, D., Wyder, T. K., Martin, D. C., et al. 2007, ApJS, 173, 315

Simard, L., Mendel, J. T., Patton, D. R., Ellison, S. L., & McConnachie, A. W. 2011, ApJS, 196, 11

Springel, V., Di Matteo, T., & Hernquist, L. 2005, ApJ, 620, L79

Strateva, I., Ivezić, Ž., Knapp, G. R., et al. 2001, AJ, 122, 1861

van den Bosch, F. C. 2002, MNRAS, 331, 98

Vikram, V., Wadadekar, Y., Kembhavi, A. K., & Vijayagovindan, G. V. 2010, MNRAS, 409, 1379

Wyder, T. K., Martin, D. C., Schiminovich, D., et al. 2007, ApJS, 173, 293

Yang, X., Mo, H. J., van den Bosch, F. C., et al. 2007, ApJ, 671, 153

Yesuf, H. M., Faber, S. M., Trump, J. R., et al. 2014, ApJ, 792, 84

York, D. G., Adelman, J., Anderson, Jr., J. E., et al. 2000, AJ, 120, 1579